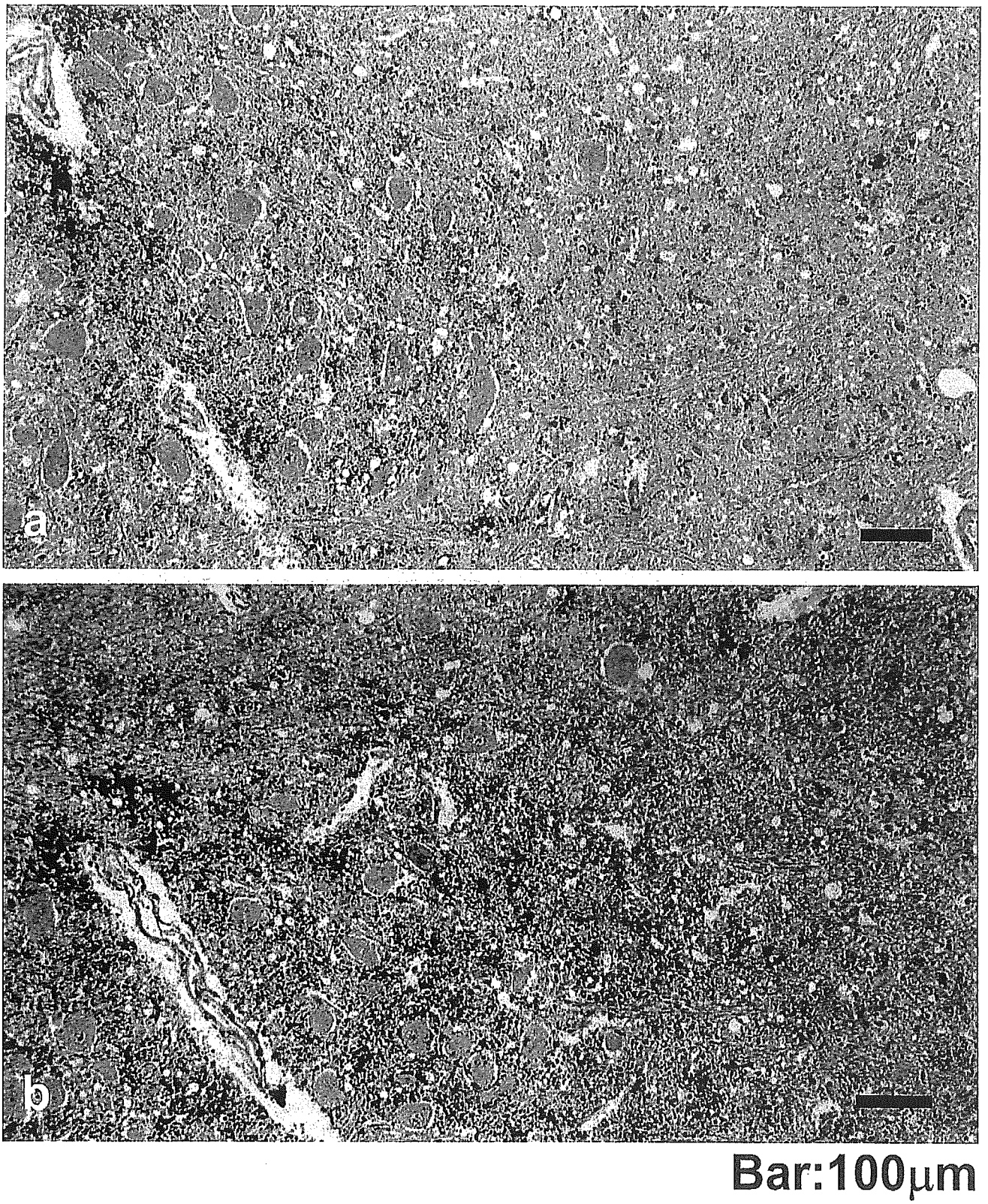

Fig. 3 Immunohistochemistry of the PrP with pAb B103 in the sections of scrapie-affected sheep from the sample immersed in formalin for 6 months; **a** 121DWHA and **b** 135DWHA methods. *Bars* **a, b** 500 μm

6 months. However, the sections treated by the 135DWHA method yielded an intense signal and widespread staining, while the detectable antigens in 121DWHA pretreatment were limited and showed low intensity (Fig. 3a, b).

Morphometry

The comparison of RD in each pretreatment method on BSE sections is shown in Fig. 4. This digital morphometry was in good agreement with the observations throughout. Although 135DWHA or 135DWHA/FA methods increased the density with mAb 43C5 and pAb B103, the effect was stronger with the former (Fig. 4a, b). Using mAbs 44B1 and 6H4, the 121DWHA/FA protocol was appropriate for antigen retrieval and the 135DWHA or 135DWHA/FA method were not effective (Fig. 4c, d).

Fig. 4 Comparison of relative density (*RD%*) using each pretreatment method on BSE sections for different antibodies; **a** pAb B103, **b** mAb 43C5, **c** mAb 6H4, and **d** mAb 44B1. mAb 44B1 recognizes discontinuous epitope, and others recognize linear epitope. The effect of FA, 121DWHA, 121DWHA/FA, 121DWHA/PK, 135DWHA and 135DWHA/FA is displayed as *bar A*, B, *C*, *D*, *E* and *F*, respectively. **a** FA displays 1 RD%. 121DWHA (29 RD%) does not lead to a significant increase. 121DWHA/FA and 121DWHA/PK show a density of 81 and 75 RD%, respectively. Immunodensity is further enhanced by 135DWHA (100 RD%) and 135DWHA/FA (100 RD%). **b** FA displays 1 RD%. 121DWHA, 121DWHA/FA and 121DWHA/PK show 15, 22 and 18 RD%, respectively. 135DWHA and 135DWHA/FA result in 100 and 94 RD%, showing a significant increase. **c** FA (5 RD%), 121DWHA (17 RD%), 121DWHA/PK (3 RD%), 135DWHA (1 RD%) and 135DWHA/FA (2 RD%) do not lead to a significant increase in immunodensity. 121DWHA/FA (100 RD%) shows the highest increase. **d** FA shows 22 RD% and 121DWHA 25 RD%. Imunodensity is not enhanced by 121DWHA/PK and 135DWHA. 135DWHA/FA displays 4 RD%. The best result was obtained by 121DWHA/FA (100 RD%) (*FA* 96% formic acid for 5 min, *121DWHA/PK* 121DWHA and proteinase K treatment for 1 min)

Discussion

In immunohistochemistry for the prion diseases, several pretreatment methods to enhance the immunoreactivity of human and animal PrP^{Sc} on the tissue sections have been reported. The method of 121°C hydrated autoclaving pretreatment or the combination method of 121°C hydrated autoclaving with a certain chemical reagent (formic acid or proteinase K, etc) are now widely used [5, 13]. The precise mechanisms by which pretreatments enhance the PrP^{Sc} immunoreactivity are still unknown. However, the effect of these chemical treatments is considered to make amyloid fibril proteins denature, breaking down the structure of amyloid fibrils, and exposing the buried epitopes [4]. In formic acid pretreatment, microwave irradiation is thought to enable for formic acid penetration in tissue, and to expose the epitope and react with the antigen more efficiently [7]. In addition, it is speculated that hydrolytic autoclaving contributes to alter the primary structures of PrP in situ [11].

We describe a new hydrated autoclaving method, termed the 135DWHA method, to enhance the immunoreactivity of the PrP^{Sc}, and have compared this with the previously reported methods. Generally, the 135DWHA or 135DWHA/FA methods for the antibodies reacting with linear epitope showed a higher

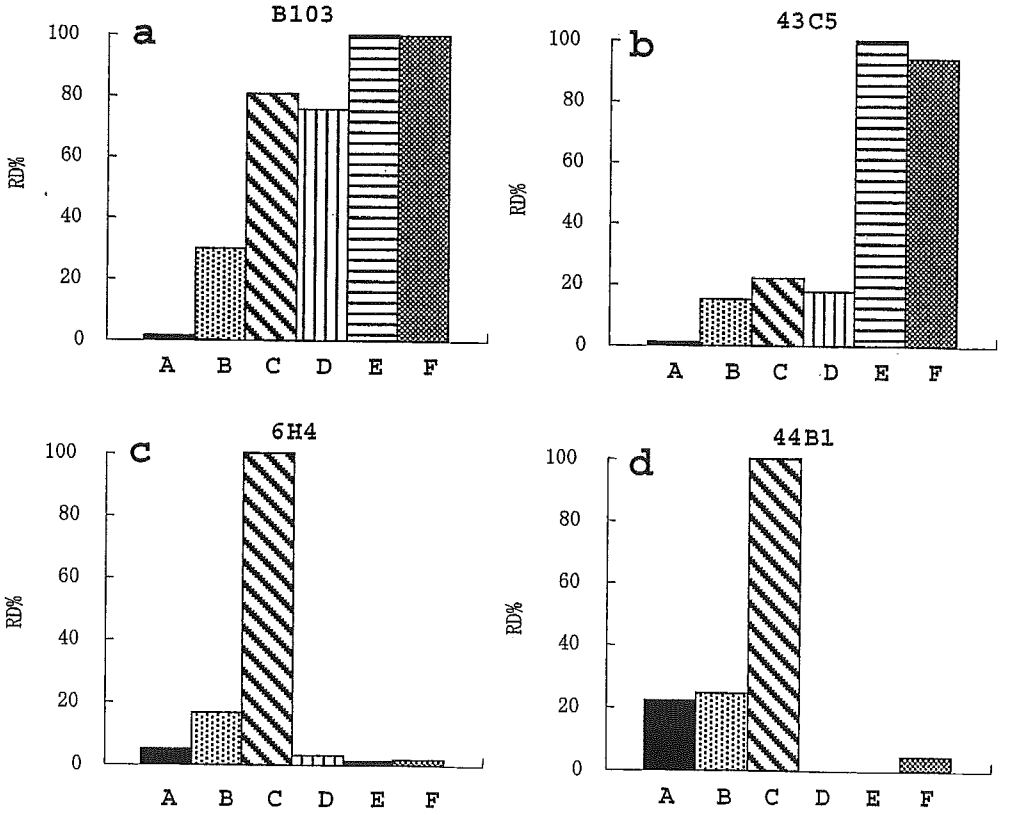

sensitivity than 121DWHA, 121DWHA/FA, or 121DWHA/PK methods, except for antibody 6H4. Although prolonged exposure of brain material to aldehyde fixatives usually dramatically decreases the antigenicity of PrP^{Sc} [17], this newly enhancing method was more effective for the long-term fixation samples compared with other methods. On the other hand, our simple modification could not enhance immunoreactivity for the prion antigen for antibodies recognizing discontinuous or conformational epitopes.

For immunohistochemical antigen-retrieval techniques, hypotheses such as breaking cross-linking [16], protein denaturation or modification-re-modification [3] have been proposed, and were thought to have an advantage on the basis of observation or support from several studies [18, 22, 23]. In particular, the later theory is based on heat- or chemical-induced modification of the three-dimensional structure of "formalinized" protein, restoring the condition of a formalin-modified protein structure back towards its original structure on the paraffin-embedding tissue sections. Because immunohistochemistry without pretreatment did not give any positive reactions using the pAb B103 and 44B1 in the frozen sections (data not shown), there are some differences between this theory and our model. However, it seemed probable that epitopes hidden by the aggregation of PrPs are exposed on the surface, or that conformational binding sites formed by the other protein molecules are disrupted due to conformational changes induced by the hydrating autoclave methods on the formalin-fixed paraffin sections, assuming that the principle of the antigen-retrieval methods is to lead to a re-naturation or partial restoration of the protein structure with re-establishment of the three-dimensional to something approaching its native condition [22, 23].

Antibody, especially that reacting on the discontinuous epitope, recognizes specific epitopes localized in a spatial configuration within the protein molecule. mAb 15B3 recognizes the discontinuous epitope in the pathological PrP isoform, and a single continuous 15B3 binding site was speculated to be formed either by aggregation of two or several PrP molecules, or by structural rearrangement of a single PrP molecule, or by a combination thereof [12]. The exact mechanisms causing the differences between 135DWHA and 121DWHA methods in the antibody's recognition of the conformational epitope are still unknown. However, these can be surmised as follows: some aggregate proteins or molecules may be loosely arranged and antigenic determinants come to lie on the surface during formic acid or 121°C, 2 atm autoclaving pretreatment; furthermore, elevation of the temperature and atmosphere may cause further changes of certain stereoscopic structures or components of PrP molecules, causing a loss of its conformational epitope. Additional formic acid treatment also causes a slight change, helping in the demasking of the conformational epitope.

Further studies on prion antigen-retrieval techniques, including establishing an exact correlation of these mechanisms and the antibody epitope, may shed new light in the pathology of the prion diseases.

Acknowledgements This work was supported by a Grant-in-Aid for Exploratory Research from the Ministry of Education, Culture, Sports, Science and Technology of Japan (grant 14656118) and a Grant from the Ministry of Health, Labor and Welfare of Japan (grant 14240101).

References

1. Bell JE, Gentleman SM, Ironside JW, McCardle L, Lantos PL, Fergusson J, Luthert P, McQuaid S, Allen IV (1997) Prion protein immunocytochemistry-UK five centre consensus report. Neuropathol Appl Neurobiol 23:26–35
2. Bodemer W (1999) The use of monoclonal antibodies in human prion disease. Naturwissenschaften 86:212–220
3. Cattoretti G, Pileri S, Parravicini C, Becker MHG, Poggi S, Bifulco C, Key G, D'Amato L, Sabattini E, Feudale E, Reynolds F, Gerdes J, Rilke F (1993) Antigen unmasking on formalin-fixed, paraffin-embedded tissue sections. J pathol 171:83–98
4. Doi-Yi R, Kitamoto T, Tateishi J (1991) Immunoreactivity of cerebral amyloidosis is enhanced by protein denaturation treatments. Acta Neuropathol 82:260–265
5. Everbroeck BV, Pals P, Martin JJ, Cras P (1999) Antigen retrieval in prion protein immunohistochemistry. J Histochem Cytochem 47:1465–1467
6. Haritani M, Spencer YI, Wells GAH (1994) Hydrated autoclave pretreatment enhancement of prion protein immunoreactivity in formalin-fixed bovine spongiform encephalopathy-affected brain. Acta Neuropathol 87:86–90
7. Hashimoto K, Mannen T, Nukina N (1992) Immunohistochemical study of kuru plaques using antibodies against synthetic prion protein peptides. Acta Neuropathol 83:613–617
8. Hayward PAR, Bell JE, Ironside JW (1994) Prion protein immunocytochemistry: reliable protocols for the investigation of Creutzfeldt-Jacob disease. Neuropathol Appl Neurobiol 20:375–383
9. Hegyi I, Hainfellner JA, Flicker H, Ironside J, Hauw JJ, Tateishi J, Haltia M, Bugiani O, Aguzzi A, Budka H (1997) Prion protein immunocytochemistry: reliable staining protocol, immunomorphology, and diagnostic pitfalls. Clin Neuropathol 16:262–263
10. Kitamoto T, Ogomori K, Tateishi J, Prusiner SB (1987) Formic acid pretreatment enhances immunostaining of cerebral and systemic amyloids. Lab Invest 57:230–236
11. Kitamoto T, Shin RW, Doh-ura K, Tomokane N, Miyazono M, Muramoto T, Tateishi J (1992) Abnormal isform of prion proteins accumulates in the synaptic structures of the central nervous system in patients with Creutzfeldt-Jakob disease. Am J Pathol 140:1285–1294
12. Korth C, Stierli B, Streit P, Moser M, Schaller O, Fischer R, Schulz-Schaeffer W, Kretzschmar H, Raeber A, Braun U, Ehrensperger F, Hornemann S, Glockshuber R, Riek R, Billeter M, Wüthrich K, Oesch B (1997) Prion (PrP^{Sc})-specific epitope defined by a monoclonal antibody. Nature 390:74–77
13. Kovács GG, Head MW, Hegyi I, Bunn TJ, Flicker H, Hainfellner JA, McCardle L, László L, Jarius C, Ironside JW, Budka H (2002) Immunohistochemistry for the prion protein: comparison of different monoclonal antibodies in human prion disease subtypes. Brain Pathol 12:1–11
14. Liberski PP, Yanagihara R, Brown P, Kordek R, Kloszewska I, Bratosiewicz J, Gajdusek DC (1996) Microwave treatment enhances the immunostaining of amyloid deposits in both the transmissible and non-transmissible brain amyloidoses. Neurodegeneration 5:95–99

15. MacDonald ST, Sutherland K, Ironside JW (1996) A quantitative and qualitative analysis of prion protein immunohistochemical staining in Creutzfeldt-Jacob disease using four anti prion protein antibodies. Neurodegeneration 5:87–94
16. Mason JT, O'Leary TJ (1991) Effects of formaldehyde fixation on protein secondary structure: a calorimetric and infrared spectroscopic investigation. J Histochem Cytochem 39:225–229
17. McBride PA, Bruce ME, Fraser H (1988) Immunostaining of scrapie cerebral amyloid plaques with antisera raised to scrapie-associated fibrils (SAF). Neuropathol Appl Neurobiol 14:325–336
18. Montero C (2003) The antigen-antibody reaction in immunohistochemistry. J Histochem Cytochem 51:1–4
19. Privat N, Sazdovitch V, Seilhean D, Laplanche JL, Hauw JJ (2000) PrP immunohistochemistry: different protocols, including a procedure for long formalin fixation, and a proposed schematic classification for deposits in sporadic Creutzfeldt-Jacob disease. Microsc Res Tech 50:26–31
20. Prusiner SB (1998) Prions. Proc Natl Acad Sci USA 95:13363–13383
21. Ryder SJ, Spencer YI, Bellerby PJ, March SA (2001) Immunohistochemical detection of PrP in the medulla oblongata of sheep: the spectrum of staining in normal and scrapie-affected sheep. Vet Rec 148:7–13
22. Shi S-R, Cote RJ, Taylor CR (1997) Antigen retrieval immunohistochemistry: past, present, and future. J Histochem Cytochem 45:327–343
23. Shi S-R, Cote RJ, Taylor CR (2001) Antigen retrieval techniques: current perspectives. J Histochem Cytochem 49:931–937
24. Wells GAH, Wilesmith JW, McGill IS (1992) Bovine spongiform encephalopathy. Brain Pathol 1:69–78

NOTE *Public Health*

Surveillance of Chronic Wasting Disease in Sika Deer, *Cervus nippon*, from Tokachi District in Hokkaido

Natsumi KATAOKA[1], Masakazu NISHIMURA[2], Motohiro HORIUCHI[3] and Naotaka ISHIGURO[4]*

[1]*Laboratories of Veterinary Public Health, and* [2]*Pharmacology, Obihiro University of Agriculture and Veterinary Medicine, Obihiro, Hokkaido 080–8555,* [3]*Laboratory of Prion Disease, Graduate School of Veterinary Medicine, Hokkaido University, Sapporo, Hokkaido 060–0813,* [4]*Laboratory of Food and Environmental Hygiene, Faculty of Applied Biological Sciences, Gifu University, Gifu 501–1193, Japan*

(Received 3 September 2004/Accepted 24 November 2004)

ABSTRACT. Surveillance of chronic wasting disease (CWD) was conducted by performing Western blot analysis of tissue samples from 136 sika deer (*Cervus nippon*) killed by hunters in the Tokachi district of Hokkaido Island. No prion protein (PrP^{Sc}) associated with CWD was detected in any of the samples. To assess amino acid polymorphisms of the sika deer PrP gene, nucleotide sequencing of the PrP gene was performed. The only amino acid polymorphisms detected were 3 silent mutations at nucleotide positions 63, 225 and 408. These results suggest that sika deer in the Tokachi district are genetically homogeneous, and are not infected with CWD.
KEY WORDS: CWD, sika deer, surveillance.

J. Vet. Med. Sci. 67(3): 349–351, 2005

Chronic wasting disease (CWD) is a transmissible spongiform encephalopathy (TSE) of captive and free-ranging white-tailed deer (*Odocoileus Virginianus*), mule deer (*O. hemionus*) and Rocky Mountain elk (*Cervus elaphus*) in several US states and Canadian provinces [13, 15, 16]. This disease is characterized by progressive loss of body weight and abnormal behavior, and by the accumulation of a partially protease-resistant isoform (PrP^{Sc}) of a normal cellular protein (PrP^{C}) in the central nervous system. Thus, CWD is similar to scrapie in sheep and goats, and bovine spongiform encephalopathy (BSE) in cattle [1, 11]. Occurrence of CWD is currently limited to North American cervid ruminants.

Cervus nippon yesoensis, a subspecies of the sika deer (*Cervus Nippon*) that inhabit the Japanese Islands, is native to Hokkaido Island of Japan. In recent decades, the number of sika deer in Hokkaido has increased rapidly due to protection by the Hokkaido government [6]. Overpopulation of sika deer has caused immense damage to agriculture and forestry in Hokkaido.

The meat of sika deer is frequently consumed as game meat or commercially processed as ham or sausage, especially in the Tokachi district of Hokkaido Island. Although there is no evidence that CWD can be transmitted to humans, the experience of transmission of other TSEs to humans via consumption of meat or other products from ruminants raises public health concerns about the safety of sika deer meat [10, 11]. However, little is known about occurrence of CWD among sika deer on Hokkaido Island. In the present study, we used Western blot analysis to examine occurrence of CWD among sika deer killed by hunters in the Tokachi district, and determined their PrP genotypes.

We used tissue samples from 136 sika deer (82 males and 54 females) killed by hunters over a 2-year period (51 deer in 2002, and 85 deer in 2003) at 13 sites in the Tokachi district (Fig. 1). The age of the deer ranged from approximately 1 to 7 years. Samples of the obex of the medulla

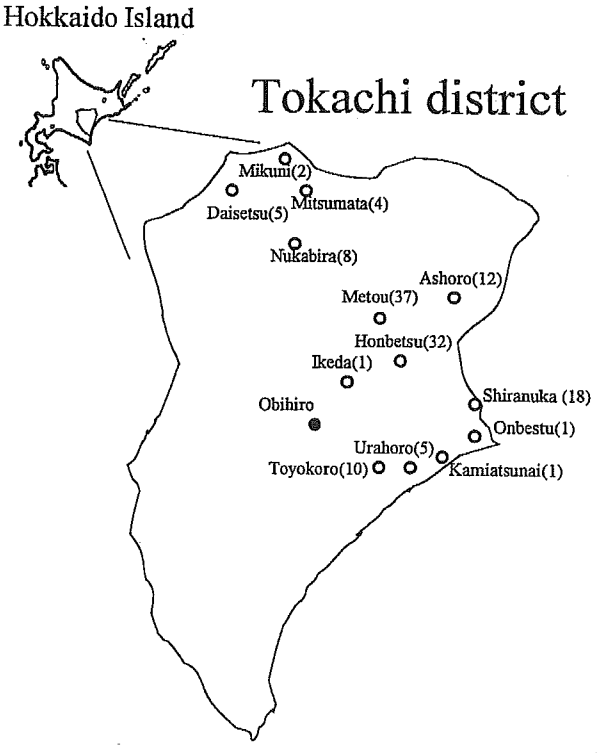

Fig. 1. Sampling sites of sika deer in Hokkaido. Tokachi district is enlarged. Numbers in parentheses are the number of sika deer killed by the hunters at each site. Obihiro city, which is indicated by a closed circle, is located at center of the Tokachi district.

* CORRESPONDENCE TO: ISHIGURO, N., Laboratory of Food and Environmental Hygiene, Faculty of Applied Biological Sciences, Gifu University, Gifu 501–1193, Japan.

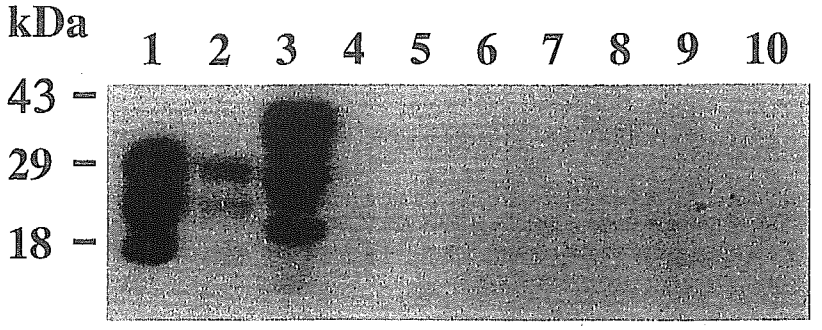

Fig. 2. Detection of PrP^{Sc} or PrP^{c} in sika deer tissue by Western blotting analysis. PrP^{c} and/or PrP^{Sc} from deer obex was prepared and dissolved in sample buffer as described previously [3]. The protein was resolved by electrophoresis in 12% polyacrylamide gels and transferred to Hybond-PVDF membranes. PrP^{Sc} and/or PrP^{c} was detected with immunoblot analysis using mAb 44B1, and was visualized using the ECL system [3]. Lane 1, PK-digested mouse PrP^{Sc} fraction of 12-μg tissue equivalent; lane 2, PK-digested mouse PrP^{Sc} fraction of 2-μg tissue equivalent; lane 3, PK-undigested PrP^{c} fraction of 2-mg tissue equivalent; lanes 4 to 10, PK-digested obex extract of 10-mg tissue equivalent. Molecular mass markers (kDa) are shown on the left.

oblongata were tested for the presence of PrP^{Sc} using Western blot analysis, and buccal muscles were tested for polymorphisms of the PrP gene by DNA sequencing. The preparation of PrP^{c} and/or PrP^{Sc} from the deer obex was performed as described elsewhere, with and without proteinase K (PK), respectively [3]. The Western blot analysis was performed as described previously, using several anti-PrP mAbs [7], and blots were developed with ECL (Amersham Buckinghamshire, England) and detected with X-ray film. PrP^{Sc} from the mouse-adapted Obihiro strain of scrapie was used as a positive control in Western blot analysis [3]. DNA was extracted from deer buccal muscle using a Dneasy Tissue Kit (Qiagen, Valencia, CA). The deer PrP gene was amplified by polymerase chain reaction (PCR) using 2 primers: BPrP3, GCAGATATAAGTCATCATGGTG; BPrP4, GGAAGGACAAAAGTGGTAGAAG [2]. The PCR products were purified using a QIAquick Kit (Qiagen), and DNA sequencing was performed as described previously [2].

To estimate the reactivity of anti-PrP mAbs to deer PrP^{c} or PrP^{Sc} molecules, the reactivity of 3 representative mAbs (132, 31C6 and 44B1, [7]) to deer PrP^{c} was examined by Western blot analysis. The mAbs 132 (which recognizes a linear epitope consisting of the amino acid sequence AVVGGLGGY) and 44B1 (which recognizes a discontinuous epitope consisting of mouse amino acid residues 155 to 231) reacted with the deer PrP^{c}, but the mAb 31C6 did not react with the deer PrP^{c} [7]. The lack of reactivity of the mAb 31C6 appears to be due to a difference in amino acid sequence between mouse and deer in the epitope region, as indicated by the DNA sequence of the deer PrP gene. Assays for deer PrP^{Sc} were performed by Western blot analysis using the mAbs 132 and 44B1. No PrP^{Sc}-specific molecules were detected in PK-treated obex extracts, although deer PrP^{c} and PrP^{Sc} from mouse-adapted scrapie (control) were observed in blots (Fig. 2).

Studies indicate that specific PrP alleles are associated with CWD in cervids [4,9]. Therefore, we examined the DNA sequences of the PrP gene in the present samples, to determine their PrP genotypes. With the exception of 3 silent mutations at nucleotide positions 63 (G→T), 255 (G→A) and 408 (C→T), the PrP sequences of the present samples were identical to the sequence with accession number AF009181 (from *Odocoileus hemionus*), and all possessed five octapeptide repeats. Specific PrP alleles were reported to be associated with CWD-positive white-tailed deer (Q^{95} G^{96} S^{138}) [4] and Rocky Mountain elk (M^{132})[9]. These amino acid sequences are observed in the wild type of sika deer PrP gene, but, it is not known if the PrP polymorphisms are associated with the occurrence of CWD in cervids on the other continents except North America [11]. No polymorphisms were observed among the present samples at the DNA level, suggesting that sika deer in Hokkaido comprise a genetically homogenous population. These results are consistent with the findings of previous mitochondrial DNA analysis [8].

There were no indications of occurrence of CWD in the present tissue samples. The number and geographical distribution of tissue samples in the present study were extremely limited. Tonsillar biopsy examined with immunohistochemical staining is a useful technique for the preclinical diagnosis of CWD in mule deer and white-tailed deer [14]. This technique might be evaluated as a practical management tool in farmed live sika deer. CWD surveillance of sika deer in the Tokachi district is important, because deer meat and other deer products are frequently consumed by humans in that area, and because sheep scrapie has been detected on farms in the Tokachi district [5, 12]. Although there is no evidence that CWD has crossed the species barrier from deer to sheep, cattle or humans [10, 11], particular care is necessary when ensuring the safety of food products

from ruminants that can carry a TSE.

ACKNOWLEDGMENTS. We wish to thank the Tokachi Hunting Club for supplying deer tissue samples. This study was supported in part by Grant-in-Aid for Scientific Research (The 21st Century Center-of-Excellence Program; E-1) from the Ministry of Education, culture, Sports, Science and Technology of Japan.

REFERENCES

1. Bolton, D.C., Mckinley, M.P. and Prusiner, S.B. 1982. *Science* **218**: 1309–1311.
2. Gombojav, A., Ishiguro, N., Horiuchi, M., Serjmyadag, D., Byambaa, B. and Shinagawa, M. 2003. *J. Vet. Med. Sci.* **65**: 75–81.
3. Gombojav, A., Shimauchi, I., Horiuchi, M., Ishiguro, N. Shinagawa, M., Kitamoto, T., Miyoshi, I., Mohri, S. and Takata, M. 2003. *J. Vet. Med. Sci.* **65**: 341–347.
4. Johnson, C., Johson, J., Clayton, M., Mckenzie, D. and Aiken, J. 2003. *J. Wildl. Dis.* **39**: 576–581.
5. Ikeda, T., Horiuchi, M., Ishiguro, N., Muramatsu, Y., Kai-Uwe, G.D. and Shinagawa, M. 1995. *J. Gen. Virol.* **76**: 2577–2581.
6. Kaji, K. 1995. *Honyurui Kagaku (Mammalian Science)* **35**: 35–43 (in Japanese).
7. Kim, C-L., Umetani, A., Matsui, T., Ishiguro, N., Shinagawa, M. and Horiuchi, M. 2004. *Virology* **320**: 41–52.
8. Nabata, D., Masuda, R. and Takahashi, O. 2004. *Zool. Sci.* **21**: 473–481.
9. O'Rourke, K.I., Besser, T.E., Miller, M.W., Cline, T.F., Spraker, T.R., Jenny, A.L., Wild, M. A., Zebarth, G.L. and Williams, E.S. 1999. *J. Gen. Virol.* **80**: 2765–2769.
10. Raymond, G.J., Bossers, A., Raymond, L.D., O'Rourke, K.I., McHolland, L.F., Bryant III, P.K., Miller, M.W., Williams, E.S., Smits, M. and Caughey, B. 2000. *EMBO J.* **19**: 4425–4430.
11. Salman, M.D. 2003. *J. Vet. Med. Sci.* **65**: 761–768.
12. Shinagawa, M., Matsuda, A., Sato, G., Takeuchi, M., Ichijo, S. and Ono, T. 1984. *Jpn. J. Vet. Sci.* **46**: 913–916.
13. Spraker, T.R., Miller, M.W., Williams, E.S., Getzy, D.M., Adrian, W.J., Schoonveld, G.G., Sponwart, R.A., O'Rourke, K.I., Miller, J.M. and Merz, P.A. 1997. *J. Wildl. Dis.* **33**: 1–6.
14. Wild, A.M., Spraker, R. T., Sigurdson, J. C., O'Rourke, I. K. and Miller, W. M. 2002. *J. Gen. Virol.* **83**: 2629–2634.
15. Williams, E.S. and Young, S. 1980. *J. Wildl. Dis.* **16**: 89–98.
16. Williams, E.S. and Young, S. 1982. *J. Wildl. Dis.* **18**: 465–471.

NOTE *Clinical Pathology*

Polymorphisms of Caprine PrP Gene Detected in Japan

Yasuhisa KUROSAKI[1], Naotaka ISHIGURO[2]*, Motohiro HORIUCHI[3] and Morikazu SHINAGAWA[4]

[1]*Laboratory of Veterinary Public Health, Obihiro University of Agriculture and Veterinary Medicine, Obihiro, Hokkaido 080–8555,* [2]*Laboratory of Food and Environmental Hygiene, Faculty of Applied Biological Sciences, Gifu University, 1–1 Yanagido, Gifu 501–1193,* [3]*Laboratory of Prion Diseases, Graduate School of Veterinary Medicine, Hokkaido University, Sapporo 060–0818 and* [4]*Prion Disease Research Center, National Institute of Animal Health, 3–1–5 Kannondai, Tsukuba, Ibaragi 305–0856, Japan*

(Received 18 August 2004/Accepted 5 November 2004)

ABSTRACT. Polymorphism of the PrP gene is a primary factor influencing susceptibility and incubation period in natural and experimental scrapie in sheep and goats. Polymorphisms of the caprine PrP gene in Japan were examined in 118 goats. Eight allelic variants and 19 genotypes were obtained. Amino acid polymorphisms were observed at 7 codons: 102, 142, 143, 240, 127, 146 and 211 (the latter 3 are novel polymorphisms). The polymorphisms at codons 142M and 143R, which are associated with the resistance to scrapie, were relatively rare in the present study. Thus, the present results provide information about the caprine PrP gene that may be useful for assessing the risk of goat scrapie.

KEY WORDS: goat, polymorphism, PrP.

J. Vet. Med. Sci. 67(3): 321–323, 2005

Scrapie is a fatal and infectious neurodegenerative disease that occurs in sheep and goats. Like bovine spongiform encephalopathy (BSE) in cattle and Creutzfeld-Jakob disease (CJD) in humans, scrapie is a transmissible spongiform encephalopathy (TSE). TSEs are characterized by accumulation of an abnormal isoform (PrP^{Sc}) of a normal cellular prion protein (PrP^{C}) in the central nervous system [12].

Among animals with natural or experimental scrapie, there is considerable variation in susceptibility and incubation period, even when the animals are exposed to the same infectious agent simultaneously [1, 4, 9]. Studies have shown that interaction between the scrapie strain and the PrP genotype in the affected animals plays a primary role in differences in infectivity [4, 8]. Polymorphisms of the open reading frame (ORF) of the cellular PrP gene significantly influence the incidence of natural scrapie [1, 9]. Amino acid polymorphisms of the sheep PrP gene have been observed at the following codons: 112 (M→T), 136 (A→V), 137 (M→T), 138 (S→N), 141 (L→F), 151 (R→C), 154 (R→H), 171 (Q→H or Q→R), 176 (K→N), and 211 (R→Q). The amino acid polymorphism at codon 171 is strongly associated with incubation period in many breeds of sheep [1, 4, 7, 9, 10, 14].

Goats as well as sheep are natural hosts for scrapie. The clinical signs of affected goats are slightly different from those of sheep, but the observed variation of incubation period is similar to that described for sheep [11, 14]. Studies have shown amino acid polymorphisms of the caprine PrP gene at the following codons: 21 (V→A), 23 (L→P), 49 (G→S), 102 (W→G), 142 (I→M), 143 (H→R), 154 (R→H), 168 (P→Q), 220 (Q→H) and 240 (S→P) [2, 3, 5, 6, 11].

In Japan, caprine scrapie has not yet been observed, although occurrence of sheep scrapie in Japan has been reported [10, 13]. In the present study, we investigated polymorphisms of the PrP gene in goats raised in Japan, to obtain genetic information for use in assessing the risk of the occurrence of scrapie in goats.

A total of 118 samples (48 tonsillar samples and 70 blood samples) were collected from healthy goats in Japan (Table 1). The 48 tonsillar samples were collected from Honshu Island, the Hachijo Islands and Hokkaido Island for TSE surveillance. The 70 blood samples were collected from goats in the Hachijo Islands (32 samples) and Okinawa Island (38 samples). Most of the goats from which samples were obtained were of the Saanen breed or related breeds.

DNA extraction from the 48 tonsillar samples and 70 blood samples was performed using the DNeasy Tissue Kit and QIAamp DNA Blood Mini Kit (QIAGEN Science, MD), respectively.

For polymerase chain reaction (PCR) and sequencing of the caprine PrP gene, the sheep primer sets SPrP-1/SP-4 and SP-1/SPrP-2 were used to amplify the upstream region (approximately 430 bp) and downstream region (approximately 370 bp) of the PrP gene, respectively [7]. The over-

Table 1. Sampling sites and caprine PrP allele variations

Sampling Sites	Number of goats	PrP allelic variants (%)
Hokkaido Island	1	1(50), 8(50)
Honshu Island	6[a)]	1(42), 2(25), 6(8), 8(25)
Hachijyo Island	73	1(44), 2(38), 5(2), 6(1), 8(15)
Okinawa Island	38	1(34), 2(33), 3(3), 4(1), 5(11), 6(8), 7(5), 8(5)

a)Aomori prefecture (3 samples), Miyagi prefecture (1 sample), Hiroshima prefecture (1 sample) and Tokyo (1 sample).

* CORRESPONDENCE TO: Dr. ISHIGURO, N., Laboratory of Food and Environmental Hygiene, Faculty of Applied Biological Sciences, Gifu University, 1–1 Yanagido, Gifu 501–1193, Japan.

Table 2. Variations of caprine PrP gene

Allele	PrP codon[a]							Number
	102	127	142	143	146	211	240	goats
1[b]	W	G	I	H	N	R	S	99
2	–	–	–	–	–	–	P	82
3	G	–	–	–	–	–	–	2
4	–	S	–	–	–	–	P	1
5	–	–	M	–	–	–	P	11
6	–	–	–	R	–	–	P	7
7	–	–	–	–	S	–	P	4
8	–	–	–	–	–	Q	–	30
Total								236
Genotype								
1/1	WW	GG	II	HH	NN	RR	SS	22
1/2	WW	GG	II	HH	NN	RR	SP	31
2/2	WW	GG	II	HH	NN	RR	PP	17
1/3	WG	GG	II	HH	NN	RR	SS	1
2/3	WG	GG	II	HH	NN	RR	SP	1
2/4	WW	GS	II	HH	NN	RR	PP	1
1/5	WW	GG	IM	HH	NN	RR	SP	4
5/8	WW	GG	IM	HH	NN	RQ	SP	1
2/5	WW	GG	IM	HH	NN	RR	PP	3
5/5	WW	GG	MM	HH	NN	RR	PP	1
5/6	WW	GG	IM	HR	NN	RR	PP	1
1/6	WW	GG	II	HR	NN	RR	SP	5
1/2	WW	GG	II	HR	NN	RR	PP	3
6/7	WW	GG	II	HR	NS	RR	PP	1
1/7	WW	GG	II	HH	NS	RR	SP	2
2/7	WW	GG	II	HH	NS	RR	PP	1
1/8	WW	GG	II	HH	NN	RQ	SS	9
2/8	WW	GG	II	HH	NN	RQ	SP	8
8/8	WW	GG	II	HH	NN	QQ	SS	6
Total								118

a) Amino acids are described as the single letter: W,tryptohan; G, glycine; S, serine; I, isoleucine; M, methionine; H, histidine; R, arginine; N, asparagine; Q, glutamine acid; P, proline.
b) Wild type of sheep.

lapping region of the 2 amplified fragments was approximately 40 bp. PCR amplification and DNA sequencing were performed as described previously [7]. To verify novel polymorphisms of the caprine PrP gene detected by direct sequencing, cloning of the caprine PrP gene to a vector plasmid was performed as described previously [7]. Five colonies possessing the recombinant plasmid were selected, and their plasmid DNAs were prepared using a Plasmid Mini Kit (QIAGEN Science) and sequenced as described previously [7].

Nine polymorphisms of the DNA sequence of the caprine PrP gene were detected (Table 2). Two of those polymorphisms (at codons 42 and 138) were silent mutations, and the remaining 7 polymorphisms (at codons 102, 127, 142, 143, 146, 211 and 240) caused amino acid changes. Three of the amino acid substitutions detected in the present study were novel polymorphisms: at codon 127, a g→a nucleotide substitution in the first codon position caused an amino acid change of G→S; at codon 146, an a→g nucleotide substitution in the second position caused an amino acid change of N→S; at codon 211, a g→a nucleotide substitution caused an amino acid change of R→Q. The remaining 4 amino acid polymorphisms detected in the present study have previously been described: codon 102, W→G; codon 142, I→M; codon 143, H→R; codon 240, S→P [2, 5, 6, 11].

The present distinctive amino acid polymorphisms at 7 codons comprised 8 allelic variations and 19 different genotypes (Table 2). Alleles 1 and 2 are the predominant alleles of the caprine PrP gene in Japan. Genotype 1/1 has been identified in wild-type sheep in Japan, and genotypes 1/2 and 2/2 are commonly observed in goats in Japan. These 3 genotype groups are distinguished by alteration of codon 240, and accounted for 59% of the 118 present samples.

To estimate the genetic background of goats from Okinawa, Hachijo, Honshu and Hokkaido Islands, allelic variants were classified along with the sampling sites (Table 1). All allelic variations detected in the present study occurred in goats from Okinawa Island. Goats from Honshu and the Hachijo Islands possessed 2 major alleles (1 and 2) and the minor alleles 5, 6 and 8. Goats in Okinawa Island have been frequently introduced from several prefectures in Honshu Island, so that allelic variants were obviously detected.

However, there have been no recent introductions of new populations of goats to the Hachijo Islands (data not shown).

The structure of the caprine PrP gene is highly homologous to that of the sheep PrP gene, including exons, the promoter region and 256 amino acids [5]. In the ORF of the PrP gene, amino acid polymorphisms associated with incubation period differ between sheep and goats. Polymorphisms at codons 142 and 143 in goats are thought to influence the incubation period of scrapie in experimental challenges [5] and natural cases [2]. Few of the goats in the present study carried polymorphisms at codons 142M or 143R (Table 2), which are associated with the resistance to scrapie. Identification of caprine PrP genotype may provide information that can be used to select scrapie-resistant goat for breeding. No scrapie has been found in goats in Japan, and PrP^{Sc} has not been found in Japan by TSE surveillance using Western blot analysis (unpublished data). Although the number of goats examined in the present study was relatively small, the present results provide useful data about variations and distribution of the caprine PrP gene, which can be used to assess the risk of scrapie in Japan.

REFERENCES

1. Belt, P. B. G. M., Muileman, I. H., Schreuder, B. E. C., Bos-de Ruijter, J., Gielkens, A. L. J. and Smits, M. A. 1995. *J. Gen. Virol.* **76**: 509–517.
2. Billins, C., Panagiotidis, C. H., Psychas, V., Argyroudis, S., Nicolaou, A., Leontides, S., Papadopoulos, O.and Sklaviadis, T. 2002. *J. Gen. Virol.* **83**: 713–721.
3. Foster, J., Goldmann, W., Parnham, D., Chong, A. and Hunter, N. 2001. *J. Gen. Virol.* **82**: 267–273.
4. Goldmann, W., Hunter, N., Smith, G., Foster, J. and Hope, J. 1994. *J. Gen. Virol.* **75**: 989–995.
5. Goldmann, W., Martin, T., Foster, J., Hughes, S., Smith, G., Hughes, K., Dawson, M. and Hunter, N. 1996. *J. Gen. Virol.* **77**: 2885–2891.
6. Goldmann, W., Chong, A., Foster J., Hope, J. and Hunter, N. 1998. *J. Gen. Virol.* **79**: 3173–3176.
7. Gombojav, A., Ishiguro, N., Horiuchi, M., Serjmyadag, D., Byambaa, B. and Shinagawa, M. 2003. *J. Vet. Med. Sci.* **65**: 75–81.
8. Hunter, N., Foster, J. D., Dickinson, A. G. and Hope, J. 1989.. *Vet. Rec.* **124**: 364–366.
9. Hunter, N., Moore, L., Hosie, B. D., Dingwall, W. S. and Greig, A. 1997. *Vet. Rec.* **140**: 59–63.
10. Ikeda, T., Horiuchi, M., Ishiguro, N., Muramatsu, Y., Kai-Uwe, G. D. and Shinagawa, M. 1995. *J. Gen. Virol.* **76**: 2577–2581.
11. Obermaier, G., Kretzschmar, H. A., Hafner, A., Heubeck, D. and Dahme, E. 1995. *J. Comp. Pathol.* **113**: 357–372.
12. Prusiner, S. B. 1991. *Science.* **252**: 1515–1522.
13. Shinagawa, M., Matsuda, A., Sato, G., Takeuchi, M., Ichijo, S. and Ono, T. 1984. *Jpn. J. Vet. Sci.* **46**: 913–916.
14. Wood, J. N. L., Done, S. H., Pritchard, G. C. and Wooldridge, M. J. A. 1992. *Vet. Rec.* **131**: 66–68.

Available online at www.sciencedirect.com
SCIENCE DIRECT®
ELSEVIER
Biochemical and Biophysical Research Communications 335 (2005) 785–792
BBRC
www.elsevier.com/locate/ybbrc

Conformational change in full-length mouse prion: A site-directed spin-labeling study

Osamu Inanami [a,f,g,*], Shukichi Hashida [a,f], Daisuke Iizuka [a], Motohiro Horiuchi [a,f], Wakako Hiraoka [b], Yuhei Shimoyama [c,g,h], Hideo Nakamura [d,g,h], Fuyuhiko Inagaki [e], Mikinori Kuwabara [a]

[a] *Laboratory of Radiation Biology, Department of Environmental Veterinary Medical Sciences, Graduate School of Veterinary Medicine, Hokkaido University, Sapporo 060-0818, Japan*
[b] *Department of Physics, School of Science and Technology, Meiji University, Kawasaki 214-8571, Japan*
[c] *Soft-Matter Physics Laboratory, Department of Materials Science and Engineering, Muroran Institute of Technology, Muroran 050-8585, Japan*
[d] *Laboratory of Chemistry, Faculty of Education, Hokkaido University of Education, Hakodate 040-8567, Japan*
[e] *Department of Structural Biology, Graduate School of Pharmaceutical Sciences, Hokkaido University, Sapporo 060-0812, Japan*
[f] *COE program, Program for Excellence of Zoonosis Control, Sapporo 060-0818, Japan*
[g] *CREST-JST, Multi-Quantum Coherence ESR Project, Muroran 050-8585, Japan*
[h] *CREST-JST, Multi-Quantum Coherence ESR Project, Hakodate 040-8567, Japan*

Received 21 July 2005
Available online 10 August 2005

Abstract

The structure of the mouse prion (moPrP) was studied using site-directed spin-labeling electron spin resonance (SDSL-ESR). Since a previous NMR study by Hornemanna et al., [Hornemanna, Korthb, Oeschb, Rieka, Widera, Wüthricha, Glockshubera, Recombinant full-length murine prion protein, mPrP (23–231): purification and spectroscopic characterization, FEBS Lett. 413 (1997) 277–281] has indicated that N96, D143, and T189 in moPrP are localized in a Cu^{2+} binding region, Helix1 and Helix2, respectively, three recombinant moPrP mutations (N96C, D143C, and T189C) were expressed in an *Escherichia coli* system, and then refolded by dialysis under low pH and purified by reverse-phase HPLC. By using the preparation, we succeeded in preserving a target cystein residue without alteration of the α-helix structure of moPrP and were able to apply SDSL-ESR with a methane thiosulfonate spin label to the full-length prion protein. The rotational correlation times (τ) of 1.1, 3.3, and 4.8 ns were evaluated from the X-band ESR spectra at pH 7.4 and 20 °C for N96R1, D143R1, and T189R1, respectively. τ reflects the fact that the Cu^{2+} binding region is more flexible than Helix1 or Helix2. ESR spectra recorded at various temperatures revealed two phases together with a transition point at around 20 °C in D143R1 and T189R1, but not in N96R1. With the variation of pH from 4.0 to 7.8, ESR spectra of T189R1 at 20 °C showed a gradual increase of τ from 2.9 to 4.8 ns. On the other hand, the pH-dependent conformational changes in N96R1 and D143R1 were negligible. These results indicated that T189 located in Helix2 possessed a structure sensitive to physiological pH changes; simultaneously, N96 in the Cu^{2+} binding region and D143 in Helix1 were conserved.

Keywords: Site-directed spin-labeling; Electron spin resonance; Prion; Conformational change; pH-sensitive region

The cellular prion protein (PrP^c) is a glycosylphosphatidylinositol (GPI)-plasma membrane-anchored protein whose function is still under debate [1–10]. Conversion of PrP^c from an α-helix- to a β-sheet-rich structure (the scrapie prion protein, PrP^{Sc}) causes relevant biophysical changes to the protein that have been related to brain dysfunction in prion diseases [1–3]. The mechanisms involved in the conversion are unknown. However, accumulating evidence suggests that

* Corresponding author. Fax: +81 11 706 7373.
E-mail address: inanami@vetmed.hokudai.ac.jp (O. Inanami).

0006-291X/$ - see front matter © 2005 Elsevier Inc. All rights reserved.
doi:10.1016/j.bbrc.2005.07.148

the process occurs after PrP^c reaches the plasma membrane, and it may involve the entry of PrP^c into intracellular acidic organelles [4–10].

As shown in Fig. 1A, the prion protein of the mouse, moPrP, consists of 208 amino acids (residues 23–231). It contains a carboxy-terminal domain, moPrP (121–231), which represents an autonomous folding unit with three α-helices (Helix1, Helix2, and Helix3) and a two-stranded antiparallel β-sheet [1–3,11–13]. In the full-length prion protein, moPrP (23–231), comparison of near-UV circular dichroism (CD), fluorescence and one-dimensional ^1H NMR spectra of moPrP (23–231) and moPrP (121–231) shows that amino-terminal segment 23–120, which includes the five characteristic octapeptide repeats, does not contribute measurably to the manifestation of the three-dimensional structure as detected [7]. Development of techniques for analysis of the structural and conformational changes in the amino-terminal region of moPrP is of great importance, because the amino-terminal region acts as a Cu^{2+} binding domain [11] and Cu^{2+} ions modulate various biological functions of prions such as the cellular enzymatic activity of superoxide dismutase (SOD) [14], signal transduction [15], shedding of PrP^c [16], and conversion to PrP^{sc} [17]. Recently, site-directed spin labeling (SDSL) together with electron spin resonance (ESR) spectroscopy has proven to be a practical method for determining the secondary structure and molecular orientation; surfaces of tertiary interactions; inter-residue distances and the chain topologies of various proteins [18–21]. SDSL involves the introduction of a spin-labeled side chain into protein sequences, usually through cysteine substitution mutagenesis, followed by reaction with a sulfhydryl-specific nitroxide reagent such as a methane thiosulfonate spin label (MTSSL) (Fig. 1B). Although SDSL-ESR is widely recognized as a useful method for structural analysis and domain dynamics of a number of membrane and soluble proteins, there are no reports about the application of this technique to detection of conformational changes in PrP^c.

In the present study, to obtain information about pH- and temperature-dependent conformational changes of typical domains in PrP, we employed the SDSL-ESR technique. We targeted the amino acid residues

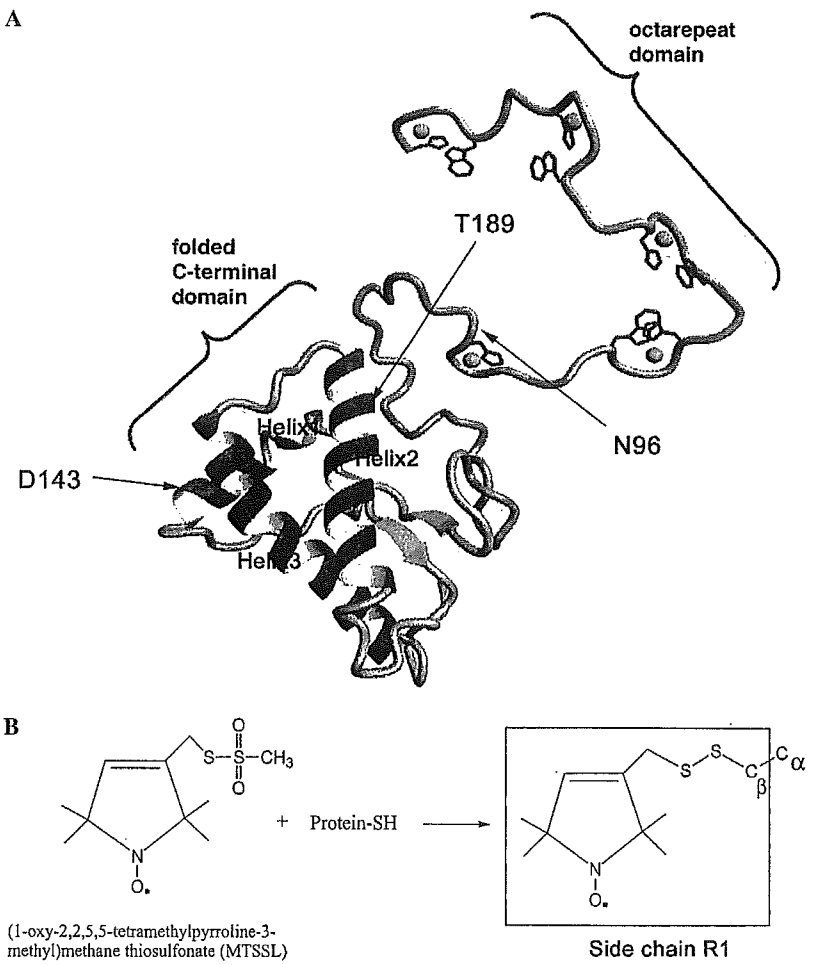

Fig. 1. (A) Three-dimensional rendering of PrP (61–231) [11] and the target sites (N96, D143, and T189) for site-directed spin-labeling (SDSL). (B) The reaction scheme of the methanethiosulfonate spin labeling reagent with cystein residue to yield the R1 side chain attached to the PrP.

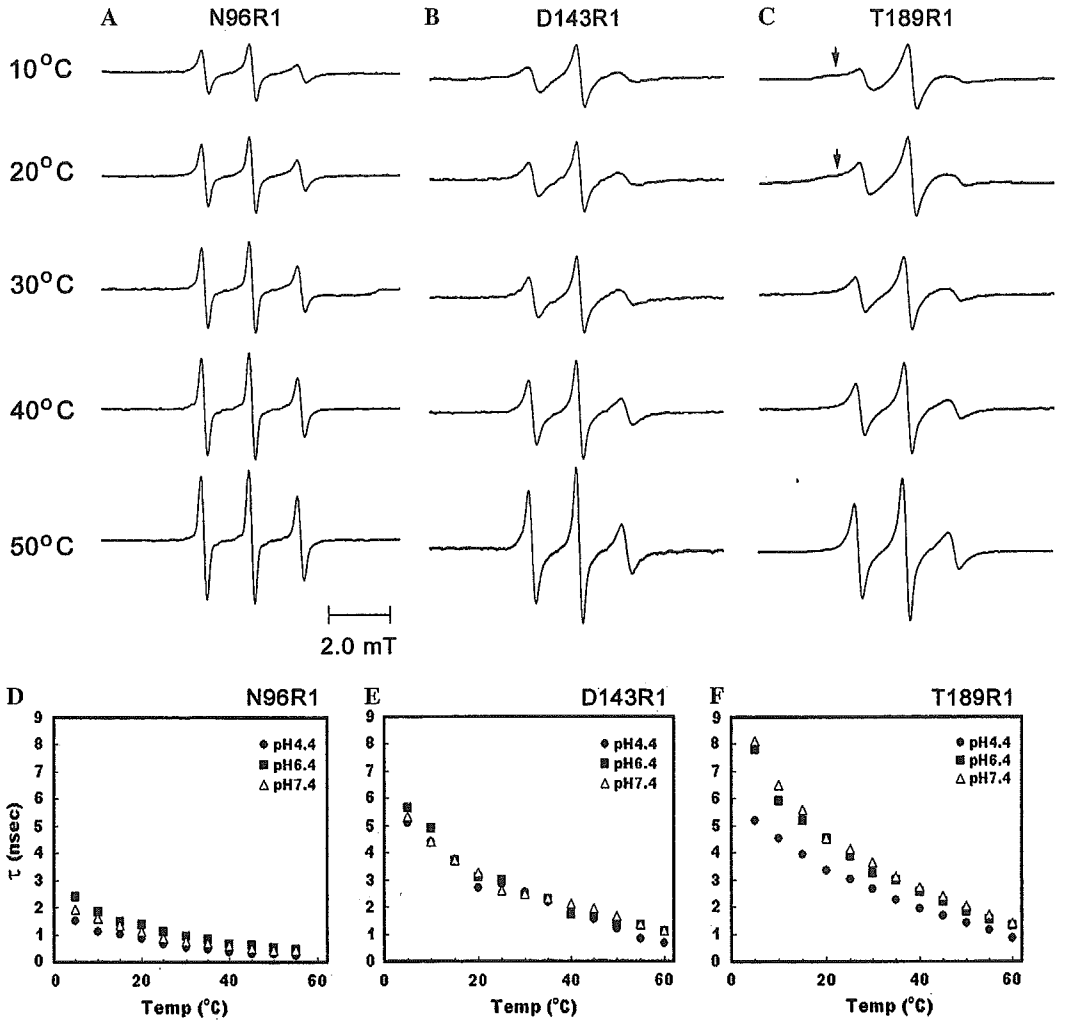

Fig. 4. X-band ESR spectra of recombinant moPrP (N96R1) (A), moPrP (D143R1) (B), and moPrP (T189R1) (C) at 10, 20, 30, 40, and 50 °C. The rotational correlation times, τ (ns), were evaluated from the ESR spectra of moPrP (N96R1) (D), moPrP (D143R1) (E), and moPrP (T189R1) (F) at various temperatures at pH 4.4, 6.4, and 7.4.

(N96C) and moPrP (D143C) as shown in Figs. 4D and E. Fig. 5 shows typical ESR spectra in pH 4.4 solution and pH 7.4 solution of moPrP (T189R1) recorded at 20 °C. The immobilization of the nitroxide moiety at pH 7.4 is obvious in comparison with that at pH 4.4. Furthermore, to define the pH-dependency, we examined the lineshape variation in the ESR spectra of moPrP (T189R1) and moPrP (T189R1) solutions whose pHs were gradually changed from pH 4.0 to 7.8 by dialysis. As shown in Fig. 5B, two regions were observable in moPrP (T189R1), a steep increase phase at pH 4.0–4.8 and a gradual increase phase at pH 5.4–7.8. Stone et al. [27] have also shown similar pH-dependent phase transition at around pH 4.0 in spin-labeled BSA. At temperatures from 5 °C to 20 °C, we found a breaking point between the two phases at around pH 5.0 that was clearer than those seen at temperatures >30 °C. These results indicated that the region around T189R1 was more pH-sensitive than the N96R1 and D189R1 regions.

Discussion

Preparation procedures of SDSL

Site-directed spin labeling is one of the most powerful methods for investigating the structure and conformational switching in soluble and membrane proteins [18,20]. Analysis of nitroxide side chain dynamics in spin-labeled proteins reveals contributions from fluctuations in the backbone, dihedral angles, and rigid-body motions of α-helices [18–21]. With this technique, however it is necessary that free cystein residues be substituted for alanine or serine residues for specificity in the reaction of MTSSL with the target cystein residue created by mutagenesis. The native mouse, hamster, bovine, and human prion proteins do not have free cystein residues, but a disulfide linkage is known to exist between Helix2 and Helix3, and to be essential for formation of three helix structures, which are important in refolding prion secondary structures [26].

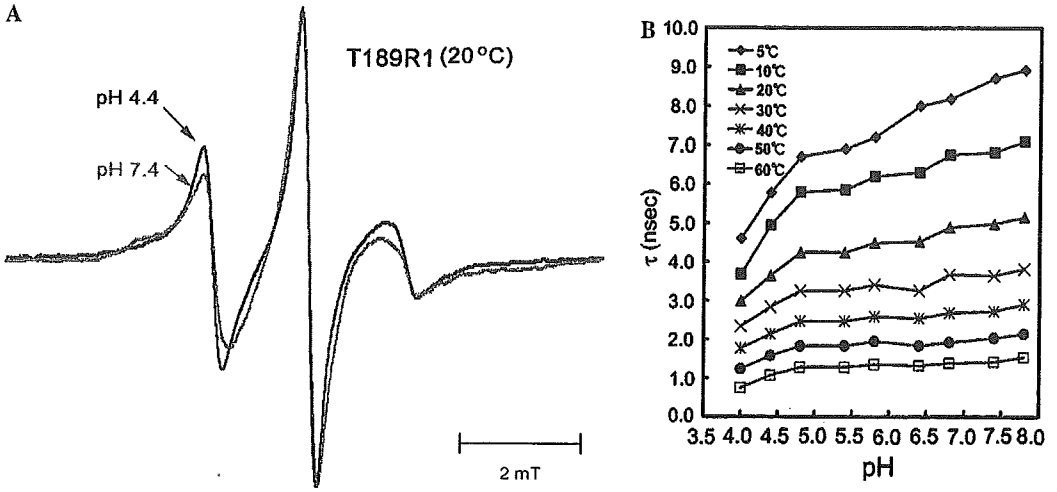

Fig. 5. (A) X-band ESR spectra of moPrP (T189R1) at 20 °C, and pH 4.4 (black line) and pH 7.4 (red line). (B) The rotational correlation time, τ (ns), at various pHs as detected by the ESR spectra of moPrP (T189R1) from 5 to 60 °C. (For interpretation of the references to colour in this figure legend, the reader is referred to the web version of this paper.)

Although Lundberg et al. [28] have reported the time-dependent changes of the ESR spectrum of a short synthetic prion-derived penta-peptide, AGAACAGA with Cys117 substituted for Ala117 in PrP (113–120), there have been few reports on structural analysis by SDSL for the full-length proteins such as PrP having an intracellular disulfide linkage. Application of the SDSL technique is impossible for full-length native PrP protein, because cystein residues newly created by mutagenesis interfere with the formation of the disulfide linkage between Helix2 and Helix3. For this reason, the present experiment employed dialysis against low pH buffer, and reverse-phase HPLC for the refolding and the purification procedures. We demonstrated that the recombinant moPrP produced by this preparation could be successfully used for SDSL experiments as proved by the following evidence. First, far-UV CD spectroscopy, as shown in Fig. 2, clearly demonstrated that the content of the helical structures in moPrP mutants was similar to that in native moPrP. This fact indicates the preferential formation of a disulfide linkage between Cys178 and Cys213, because the abrogation of this disulfide linkage never gives two minima at 208 and 220 nm in far-UV CD spectra [26]. Second, the possibility of dimer formation due to intermolecular disulfide-linkage between cystein residues newly created by mutagenesis was ruled out because SDS–PAGE of recombinant moPrP without the reducing reagent showed a single band (data not shown). Third, MALDI-TOF mass spectroscopic data showed increases of ca. $m/z = 184$ due to a side chain of the nitroxide moiety in the fragment after the tryptic digestion of spin-labeled moPrP mutants (data not shown). Thus, we were able to preserve the target cystein created by mutagenesis and succeeded for the first time in applying SDSL to the full-length prion protein.

Conformational changes of Cu^{2+} binding region and α-helix regions

Prion protein was reported to contain an amino-terminal Cu^{2+} binding octarepeat segment and a carboxy-terminal domain, three α-helices (Helix1, Helix2, and Helix3), and a two-stranded antiparallel β-sheet [1–3,11–13]. The amino acid residues of N96, D143, and T189 in moPrP have been chosen as targets for SDSL. Recently, in addition to the octapeptide repeat region, a novel Cu^{2+} binding structure between H95 and H110 was reported [29] and N96 is close to this region. D143 is located in the initial part of Helix1 and D189 in the end part of Helix2. A marked difference in rotational correlation times was observed by the spin-labeled positions (Fig. 3). NMR data of hamster PrP (90–231) showed that the region from 90 to 124, which includes the characteristic octapeptide repeat sequence, was clearly flexible with large negative NOEs and local correlation times of less than 1 ns. This is due to the fact that residues do not form part of any stable secondary or tertiary fold and are highly flexible [30]. Our ESR spectrum of moPrP (N96R1) also showed that the Cu^{2+} region around H95 reflected more flexible motion as compared with the rigid-body motion of helix structure revealed by ESR-lineshapes from moPrP (D143R1) and moPrP (T189R1).

Our data showed that the end part of Helix2 around T189R1 was highly pH-sensitive compared to the Cu^{2+} binding region around N96R1 and the first part of Helix1 around T189R1 (Figs. 4D–F and 5). The conversion from PrP^{c} to PrP^{Sc} is a post-transcriptional process that appears via the endosome pathway [4,5,9] and/or caveolae-like domains [10], both of which are acidic. Lower pH also accelerates conversion from

PrP^{c} to PrP^{Sc} in a cell-free system [31]. Recently, Swietnicki et al. [32] have shown that incubation of the recombinant prion protein under mildly acidic conditions (pH 5 or below) in the presence of low concentrations of guanidine hydrochloride produces a transition to PrP^{Sc}-like β-sheet-rich oligomers that show fibrillar morphology and increased resistance to proteinase K digestion. Since low pH plays a role in facilitating the conformational change that ultimately results in PrP^{Sc} formation, some parts of Helix2 may be candidates for the pH-sensitive region associated with PrP^{Sc} conversion. In this region, we found a phase transition point at around pH 5.0 as shown in Fig. 5B. This evoked the induction of rapid structural change in the end part of Helix2 below pH 5.0. For analysis of the precise mechanism of pH-induced conformational changes in this region, further studies using the SDSL-ESR technique using a variety of recombinant moPrP mutants created on Helix2 will be necessary.

ESR of spin label dynamics

The mobility of the spin label moiety attached to a protein can be quantified in terms of the rotational correlation times in the case of weakly immobilized labels ($\tau = 10^{-9}$–10^{-10} s). τ is determined by the relative linewidths based upon relaxation theory and is given by Eq. (1) (vide infra). In the equation, the lineheights are used instead of the linewidths, because the former are easy to measure accurately. The constant factor a_0 in Eq. (1) is derived from the g-factor and hyperfine anisotropies. For these reasons, Eq. (1) is only applicable to a spin label signal that possesses three well-defined lines with longitudinal (or up and down) symmetry and no anisotropic outermost lines due to the $g_{\|}$ anisotropy. In the present study, we applied Eq. (1) to the rapid tumbling of the weakly immobilized regime of the spin label dynamics.

Acknowledgments

This work was supported in part by Grants-in-Aid for Basic Scientific Research from the Ministry of Education, Culture, Sports, Science and Technology of Japan [No. 17380178 (O.I.), No. 17580275, and No. 17658126 (M.K.)]. O.I., Y.S., and H.N. thank the Research Grants from COE program and CREST-JST program.

References

[1] S.B. Prusiner, Prions, Proc. Natl. Acad. Sci. USA 95 (1998) 13363–13383.
[2] C. Weissmann, Molecular genetics of transmissible spongiform encephalopathies, J. Biol. Chem. 274 (1999) 3–6.
[3] A. Aguzzi, M. Glatzel, F. Montrasio, M. Prinz, F.L. Heppner, Interventional strategies against prion diseases, Nat. Rev. Neurosci. 2 (2001) 745–749.
[4] B. Caughey, G.J. Raymond, The scrapie-associated form of PrP is made from a cell surface precursor that is both protease- and phospholipase-sensitive, J. Biol. Chem. 266 (1991) 18217–18223.
[5] B. Caughey, G.J. Raymond, D. Ernst, R.E. Race, N-terminal truncation of the scrapie-associated form of PrP by lysosomal protease(s): implications regarding the site of conversion of PrP to the protease-resistant state, J. Virol. 65 (1991) 6597–6603.
[6] A. Taraboulos, M. Scott, A. Semenov, D. Avrahami, L. Laszlo, S.B. Prusiner, D. Avrahami, Cholesterol depletion and modification of COOH-terminal targeting sequence of the prion protein inhibit formation of the scrapie isoform, J. Cell Biol. 129 (1995) 121–132.
[7] S. Hornemanna, C. Korthb, B. Oeschb, R. Rieka, G. Widera, K. Wüthricha, R. Glockshubera, Recombinant full-length murine prion protein, mPrP (23–231): purification and spectroscopic characterization, FEBS Lett. 413 (1997) 277–281.
[8] A.C. Magalhaes, J.A. Silva, K.S. Lee, V.R. Martins, V.F. Prado, S.S. Ferguson, M.V. Gomez, R.R. Brentani, M.A. Prado, Endocytic intermediates involved with the intracellular trafficking of a fluorescent cellular prion protein, J. Biol. Chem. 277 (2002) 33311–33318.
[9] D.R. Borchelt, A. Taraboulos, S.B. Prusiner, Evidence for synthesis of scrapie prion proteins in the endocytic pathway, J. Biol. Chem. 267 (1992) 16188–16199.
[10] M. Vey, S. Pilkuhn, H. Wille, R. Nixon, S.J. DeArmond, E.J. Smart, R.G. Anderson, A. Taraboulos, S.B. Prusiner, Subcellular colocalization of the cellular and scrapie prion proteins in caveolae-like membranous domains, Proc. Natl. Acad. Sci. USA 93 (1996) 14945–14949.
[11] C.S. Burns, E. Aronoff-Spencer, G. Legname, S.B. Prusiner, W.E. Antholine, G.J. Gerfen, J. Peisach, G.L. Millhauser, Copper coordination in the full-length, recombinant prion protein, Biochemistry 42 (2003) 6794–6803.
[12] M. Billeter, R. Riek, G. Wider, S. Hornemann, R. Glockshuber, K. Wuthrich, Prion protein NMR structure and species barrier for prion diseases, Proc. Natl. Acad. Sci. USA 94 (1997) 7281–7285.
[13] R. Riek, S. Hornemann, G. Wider, M. Billeter, R. Glockshuber, K. Wuthrich, NMR structure of the mouse prion protein domain PrP (121–321), Nature 382 (1996) 180–182.
[14] W. Rachidi, D. Vilette, P. Guiraud, M. Arlotto, J. Riondel, H. Laude, S. Lehmann, A. Favier, Expression of prion protein increases cellular copper binding and antioxidant enzyme activities but not copper delivery, J. Biol. Chem. 278 (2003) 9064–9072.
[15] C. Spielhaupter, H.M. Schatzl, PrP^{C} directly interacts with proteins involved in signaling pathways, J. Biol. Chem. 276 (2001) 44604–44612.
[16] E.T. Parkin, N.T. Watt, A.J. Turner, N.M. Hooper, Dual mechanisms for shedding of the cellular prion protein, J. Biol. Chem. 279 (2004) 11170–11178.
[17] N. Hijazi, Y. Shaked, H. Rosenmann, T. Ben-Hur, R. Gabizon, Copper binding to PrP^{C} may inhibit prion disease propagation, Brain Res. 993 (2003) 192–200.
[18] W.L. Hubbell, C. Altenbach, C.M. Hubbell, H.G. Khorana, Rhodopsin structure, dynamics, and activation: a perspective from crystallography, site-directed spin labeling, sulfhydryl reactivity, and disulfide cross-linking, Adv. Protein Chem. 63 (2003) 243–290.
[19] R. Biswas, H. Kuhne, G.W. Brudvig, V. Gopalan, Use of EPR spectroscopy to study macromolecular structure and function, Sci. Prog. 84 (2001) 45–67.
[20] W.L. Hubbell, D.S. Cafiso, C. Altenbach, Identifying conformational changes with site-directed spin labeling, Nat. Struct. Biol. 7 (2000) 735–739.

[21] H.S. Mchaourab, M.A. Lietzow, K. Hideg, W.L. Hubbell, Motion of spin-labeled side chains in T4 lysozyme. Correlation with protein structure and dynamics, Biochemistry 35 (1996) 7692–76704.
[22] C.L. Kim, A. Umetani, T. Matsui, N. Ishiguro, M. Shinagawa, M. Horiuchi, Antigenic characterization of an abnormal isoform of prion protein using a new diverse panel of monoclonal antibodies, Virology 320 (2004) 40–51.
[23] Y. Imai, Y. Mastushima, T. Sugimura, M. Terada, A simple and rapid method for generating a deletion by PCR, Nucleic Acid Res. 19 (1991) 2785.
[24] J. Sambrook, E.F. Fritsch, T. Maniatis, Molecular Cloning: A Laboratory Manual, Cold Spring Harbor Press, Cold Spring Harbor, NY, 1989.
[25] D. Kivelson, Theory of ESR linewidths of free radicals, J. Chem. Phys. 33 (1960) 1094–1106.
[26] N.R. Maiti, W.K. Surewicz, The role of disulfide bridge in the folding and stability of the recombinant human prion protein, J. Biol. Chem. 276 (2001) 2427–2431.
[27] T.J. Stone, T. Buckman, P.L. Nordio, H.M. McConnel, Spin-labeled biomolecules, Proc. Natl. Acad. Sci. USA 54 (1965) 1010–1017.
[28] K.M. Lundberg, C.J. Stenland, F.E. Cohen, S.B. Prusiner, G.L. Millhauser, Kinetics and mechanism of amyloid formation by the prion protein H1 peptide as determined by time-dependent ESR, Chem. Biol. 4 (1997) 345–355.
[29] C.E. Jones, S.R. Abdelraheim, D.R. Brown, J.H. Viles, Preferential Cu^{2+} coordination by His96 and His111 induces beta-sheet formation in the unstructured amyloidogenic region of the prion protein, J. Biol. Chem. 279 (2004) 32018–32027.
[30] H. Liu, S. Farr-Jones, N.B. Ulyanov, M. Llinas, S. Marqusee, D. Groth, F.E. Cohen, S.B. Prusiner, T.L. James, Solution structure of Syrian hamster prion protein rPrP (90–231), Biochemistry 38 (1999) 5362–5377.
[31] D.A. Kocisko, S.A. Priola, G.J. Raymond, B. Chesebro, P.T.Jr. Lansbury, B. Caughey, Species specificity in the cell-free conversion of prion protein to protease-resistant forms: a model for the scrapie species barrier, Proc. Natl. Acad. Sci. USA 92 (1995) 3923–3927.
[32] W. Swietnicki, M. Morillas, S.G. Chen, P. Gambetti, W.K. Surewicz, Aggregation and fibrillization of the recombinant human prion protein huPrP90–231, Biochemistry 39 (2000) 424–431.

Neuroradiology (2005) 47: 501–506
DOI 10.1007/s00234-005-1372-x

Akio Soeda
Toshihiko Nakashima
Ayumi Okumura
Kazuo Kuwata
Jun Shinoda
Toru Iwama

Cognitive impairment after traumatic brain injury: a functional magnetic resonance imaging study using the Stroop task

Received: 15 October 2004
Accepted: 31 January 2005
Published online: 23 June 2005

A. Soeda (✉) · T. Iwama
Department of Neurosurgery,
Gifu University School of Medicine,
1-1 Yanagido, Gifu City 501-1194, Japan
E-mail: ccd29400@nyc.odn.ne.jp
Tel.: +81-58-2306271
Fax: +81-58-2306272

T. Nakashima · A. Okumura · J. Shinoda
Chubu Medical Center for Prolonged
Traumatic Brain Dysfunction,
Department of Neurosurgery, Kizawa
Memorial Hospital, Minokamo, Japan

K. Kuwata
Department of Biochemistry and
Biophysics, Gifu University School of
Medicine, Gifu, Japan

Abstract The anterior cingulate cortex (ACC) plays a key role in cognition, motor function, and emotion processing. However, little is known about how traumatic brain injury (TBI) affects the ACC system. Our purpose was to compare, by functional magnetic resonance imaging (fMRI) studies, the patterns of cortical activation in patients with cognitive impairment after TBI and those of normal subjects. Cortical activation maps of 11 right-handed healthy control subjects and five TBI patients with cognitive impairment were recorded in response to a Stroop task during a block-designed fMRI experiment. Statistical parametric mapping (SPM99) was used for individual subjects and group analysis. In TBI patients and controls, cortical activation, found in similar regions of the frontal, occipital, and parietal lobes, resembled patterns of activation documented in previous neuroimaging studies of the Stroop task in healthy controls. However, the TBI patients showed a relative decrease in ACC activity compared with the controls. Cognitive impairment in TBI patients seems to be associated with alterations in functional cerebral activity, especially less activation of the ACC. These changes are probably the result of destruction of neural networks after diffuse axonal injury and may reflect cortical disinhibition attributable to disconnection or compensation for an inefficient cognitive process.

Keywords Cognitive function · Functional MRI · Brain injury · Stroop task

Introduction

Follow-up studies of patients with traumatic brain injury (TBI) disclosed cognitive dysfunction even in patients with good neurological recovery [1–5]. In spite of advances in acute care and rehabilitation, these deficits interfere with the rehabilitation process, social re-integration, and the ability to function independently.

Several neuroimaging studies revealed structural, cerebral blood flow, and metabolic abnormalities following TBI [2, 3], such as corpus callosal atrophy [4] and anterior temporal dysfunction [5]. However, these studies assessed the patient at resting condition, a status in which neural activity is different from task-related neural activity. Positron-emission tomography (PET) or functional magnetic resonance imaging (fMRI) has been applied to assess changes in neural circuitry in response to specific tasks with well-described functional neuroanatomical characteristics [6]. For example, in an fMRI study of working memory, TBI patients showed increased activation of right frontal regions and generally increased dispersion of activation [7]. In a PET study, they manifested reduced frontal activation during free recall and increased frontal activation during recognition [8]. However, in those studies, working memory tasks that stress these networks were used, and

other cognitive functions, such as attention and emotional disorders, were not taken into consideration.

Psychological studies indicated that cognitive impairment was related to frontal and anterior cingulate cortex (ACC) abnormalities [9, 10], and fMRI studies provided information regarding the role of the ACC during the Stroop task [11–15]. This task is a classical experimental paradigm used in cognitive neuroscience to probe attention phenomena [16]. These studies showed that the ACC played a key role in selective attention, motor function, and emotional processing. However, little is currently known about how the ACC system is disrupted by TBI. Statistical analysis showed that the Stroop task was better at discriminating between TBI and control groups than other neuropsychological tests were [17]. To our knowledge, no neuroimaging studies on TBI patients performing the Stroop task have been published to date.

In this fMRI study, we tested our hypothesis that ACC dysfunction contributes to cognitive impairment in individuals with TBI. To this end, we compared the patterns of cortical activation during the Stroop task in TBI patients and healthy subjects.

Methods

Participants

The study population consisted of five patients, three men and two women aged between 24 years and 38 years (mean 29.8 ± 6.4 years), who were making a good neurological recovery after sustaining a severe closed head injury caused by motor vehicle accident. Severe head injury was defined as an initial Glasgow coma scale (GCS) score between 3 and 8 [18]. Initial MRI revealed small focal and diffuse neuropathological consequences, typical of moderate-to-severe TBI, in all patients. There was no evidence of massive contusions, including to the ACC, and none of the patients underwent surgical procedures. All underwent neuropsychological testing by the 30-point mini-mental state examination (MMSE) [19], the Wechsler adult intelligence scale-revised (WAIS-R) [20], and the Wechsler memory scale-revised (WMS-R) [21]; all tests were the Japanese-language version. A trained neuropsychological technician, blind to the MRI findings, administered the neuropsychological tests. These tests and fMRI were performed between 1 year and 7 years after the injury. Clinical and neuropsychological data are summarized in Table 1. Patients were compared with 11 age-matched and education-matched right-handed healthy subjects, seven men and four women aged between 23 years and 35 years (mean 28.1 ± 4.7 years). All control subjects were screened to ensure that they had no history of neurological damage or color-blindness. Written prior informed consent, approved by the Gifu University Medical Review Board, was obtained from all study subjects before inception of this investigation.

Task and design

We used a modified Japanese-language version of the Stroop test. The following two variants of the Stroop task were assigned [13]: (1) the color-naming Stroop task, in which the displayed word named the ink color of the word, and selected name color cards (e.g., the word "yellow" printed in green selects the green card); (2) the word-naming Stroop task, in which the displayed word named a color that was different from that of its ink color, and selected name color cards (e.g., the word "blue" printed in red selects the blue card). The colors used were red, blue, green, and yellow. The stimuli were shown by fiber-optic glasses (Silent Vision 4000, Avotec, USA). Each stimulated block consisted of 15 trials, presented at a rate of one trial every 2 s. The subjects responded by pressing right/left buttons in response to color-congruent/word-congruent targets [12]. A scanner was used to obtain accuracy data for all subjects. We were not able to record reaction time data during scanning.

Functional MRI procedure

We used a blocked fMRI design that involved presentation of a 30-s rest condition followed by a 30-s activation condition. This cycle was repeated three times over the course of 3 min. The resting baseline reference task was a standard condition during which subjects were instructed to lie still and remain quiet with their eyes open [22]. Functional and anatomical imaging was performed on a 1.5 T clinical scanner (Signa, GE Medical Systems, Milwaukee, Wis., USA) with a standard head coil. Blood oxygenation level-dependent (BOLD) functional images parallel to the bicommissural plane were acquired with single-shot echo planar sequences (repetition time 3,000 ms, echo time 50 ms, flip angle 90°, acquisition matrix 64×64, field of view 24 cm, 15 slices, slice thickness 7 mm, slice gap 1.5 mm). In addition, high-resolution T1-weighted three-dimensional spoiled gradient echo (SPGR) anatomical images were obtained (repetition time 7.2 ms, echo time 1.5 ms, flip angle 10°, acquisition matrix 256 ×256, field of view 24 cm, 160 slices, slice thickness 1 mm). During each cognitive task condition, 60 images per slice were acquired in 210 s (total = 960 images).

Table 1 Subject characteristics (*FSIQ* full-scale intelligence quotient, *VIQ* verbal IQ, *PIQ* performance IQ, *NA* not available)

Characteristic	TBI patients							Controls (n = 11)		*P*
	1	2	3	4	5	Mean	SD	Mean	SD	
Age/gender	28/F	24/M	38/F	35/M	24/M	29.8	6.4	28.1	4.7	0.78
Education (years)	14	12	12	16	14	13.6	1.7	14.6	1.3	0.73
Time to test (months)	54	12	24	84	48	45.6	28.7	NA	NA	
MMSE[a]	30	25	29	30	30	29.8	0.5	NA	NA	
WAIS-R										
FSIQ	86	70	100	90	65	82.2	14.5	NA	NA	
VIQ	85	86	89	93	73	85.2	7.5	NA	NA	
PIQ	91	57	114	88	65	83.0	22.6	NA	NA	
WMS-R										
Logical memory	84	54	93	65	62	71.6	16.3	NA	NA	
Attention	82	87	92	102	82	89.0	8.4	NA	NA	
Visual reproduction	69	69	88	65	69	72.0	9.1	NA	NA	
Stroop[b]	78	80	76	82	71	77.4	4.2	98.0	1.6	0.51

Data analysis

Post-processing was done on a Microsoft workstation using SPM99 (The Welcome Department of Neurology, University College London, UK) implemented in Matlab (Mathworks, Sherborn, Mass., USA). Realignment for motion correction, normalization, and deformation was performed by using the standard brain template from the Montreal Neurological Institute (MNI) and converting to the space of the stereotactic atlas of Talairach and Tournoux [23]. Smoothing was at 10-mm thickness; for data analysis we used thresholds of $P < 0.05$ (corrected) for individual subjects.

Using these data we calculated group activation maps by pooling the data for each condition at thresholds of $P < 0.001$ (uncorrected). The output from each statistical analysis is a statistical parametric map or a three-dimensional image.

Results

Behavioral data

Control subjects and TBI patients did not differ significantly with respect to gender, age, and years of education. Although the TBI patients did generally as well as the control subjects, they manifested a poor memory for recent events and had trouble with their jobs. Although the patients were able to perform the Stroop task, they made more errors than the controls; however, there was not a significant difference between the two groups ($P = 0.51$).

Imaging data

Follow-up MRI scans showed cerebral abnormalities in two patients. Patient 4 in Table 1 had a small contusion scar at the bilateral frontal cortices and patient 1 had a slight subdural effusion in the right frontal region. There was no evidence of abnormalities in the other three patients.

The location of significant increases in the BOLD signal during the modified Stroop task is shown in Table 2 and Fig. 1. In TBI patients and controls, cortical activation was found in similar regions of the frontal [Broadmann's area (BA) 6, 44, 46], occipital (BA 19, 37), and parietal (BA 7, 40) lobes and resembled the patterns of activation documented in previous neuroimaging studies of the Stroop task in healthy non-Japanese controls [12, 13, 15], indicating that our modified Japanese version of the computed Stroop task can be used to evaluate cerebral recruitment in Japanese subjects.

As shown in Fig. 2, compared to the control group, the TBI group displayed more relatively decreased cerebral activation in the ACC (BA 32).

Discussion

Using fMRI studies, we compared the pattern of cortical activation in patients with TBI and healthy control subjects. Although cognitive impairment may be subclinical and discrete in TBI patients, it can pose considerable challenges in their social re-integration [1]. Our results provide results of our interrogation of cortical physiology after head injury.

Table 2 Comparison of the location of significant increases in BOLD signal during the modified Stroop task performed by TBI patients and healthy subjects

Region	Size of voxels	Coordinates (mm)			*Z* score
		x	*y*	*z*	
Controls					
Right anterior cingulate and medial frontal gyrus (BA 6, 32)	1,904	2	−2	58	6.48
		2	18	46	5.71
Left inferior parietal gyrus and precuneus (BA 7, 19, 40)	4,292	−24	−90	16	6.28
		−32	−62	52	5.93
Right inferior parietal gyrus and precuneus (BA 19, 40)	2,290	34	−76	30	6.06
		46	−54	52	5.74
		34	−68	38	5.62
Left middle and inferior frontal gyrus (BA 44, 46)	865	−44	42	22	5.75
		−44	18	26	4.32
Right inferior parietal and precuneus (BA 19, 37)	2,386	−48	8	34	3.46
		50	−66	−16	5.69
		56	−54	−12	5.40
Right middle frontal gyrus (BA 6)	527	36	−4	52	4.70
Right inferior frontal gyrus (BA 10, 46)	194	48	36	22	3.73
		40	50	22	3.65
Left middle frontal gyrus (BA 6)	117	−28	−10	56	3.63
Patients with TBI					
Left inferior frontal gyrus (BA 45)	93	−56	18	8	5.14
Left middle frontal gyrus (BA 6)	442	−48	4	24	4.67
Right middle and inferior frontal gyrus (BA 6, 9, 44)	227	40	8	26	4.21
		52	8	42	3.81
		44	4	34	3.44
Right inferior parietal gyrus (BA 40)	197	36	−64	42	4.13
Right medial frontal gyrus (BA 6)	77	10	4	54	3.95

The cingulate cortex is comprised of the anterior and posterior cortices, each of which possesses different thalamic and cortical connections [9]. The ACC can be divided into discrete anatomic and behavioral subdivisions: the affective division (ACed) and the cognitive division (ACcd) [14]. The ACed includes areas 25, 33, and rostal area 24 and plays a role in emotion and motivation; the ACcd includes caudal areas 24 and 32 and plays a role in complex cognitive/attentional processing [10, 11, 14]. Neuroimaging studies have shown that the ACcd is activated by numerous cognitive/attentional tasks including Stroop tasks, divided attention tasks, and working memory tasks [12, 24, 25]. The ACcd is vitally important for the proper and efficient functioning of frontostriatal attention networks.

One key region of working memory is the prefrontal cortex, and, in patients with TBI, the frontal cortices tend to be damaged both structurally and functionally

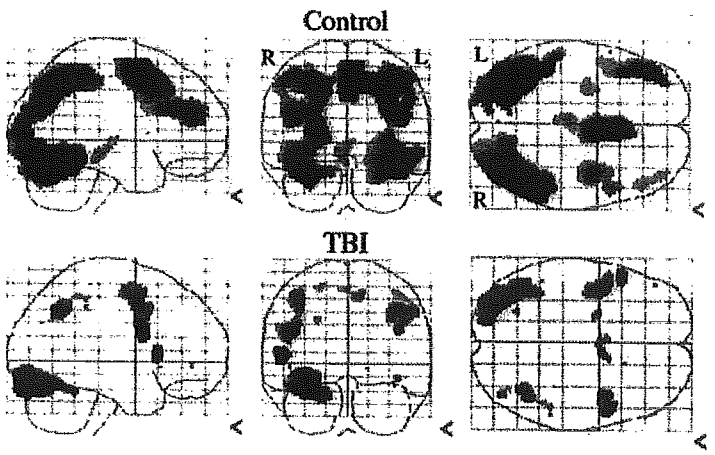

Fig. 1 Maximum-intensity projections of the statistical parametric maps during the Stroop task for TBI patients (*bottom*) and healthy controls (*top*) ($P < 0.001$, uncorrected). For localization of activation see Table 1